INVESTIGATION OF A HYDROGEN PLASMA WITH "HOT" ELECTRONS

É. Z. TARUMOV, Yu. L. BAKSHAEV, V. L. BORZENKO, V. S. PEN'KINA, and V. I. ROZANOVA

Submitted to JETP editor July 16, 1966

J. Exptl. Theoret. Phys. (U.S.S.R.) 52, 49—65 (January, 1967)

Results are reported of an experimental investigation of the characteristics of a discharge plasma with hot electrons ($n_h \sim 10^{11}$ cm^{-3}, $T_{eh} \sim 100$ keV, $n_e T_{e\perp} 6 \times 10^{15}$ eV/cm^3). The discharge was excited in hydrogen at a pressure $\lesssim 10^{-4}$ mm Hg by an electron beam of 5—6 keV energy and 2—3 A current, injected along a magnetic mirror trap ($H_{mir}/H_0 \approx 4$, $H_0 = 1200$ Oe) in the stationary and pulsed modes. The characteristics of the decay plasma were investigated in the pulsed mode. Simultaneous use of several measurement procedures (x-rays, microwaves, light, diamagnetic probe) has made it possible to increase the degree of reliability of the results. It is established that the density of the "hot" electrons amounts to 1/10 of the total plasma density in the discharge and to 1/3 in the decay part. It is shown that the discharge plasma contains three groups of electrons: "hot" ($T_{eh} \sim 100$ keV), "warm" ($T_{ew} \sim 100$ eV), and "cold" ($T_{ec} \sim 4$ eV). In the decay plasma there are two groups, "hot" and "cold."

1. INTRODUCTION

THE instability of an electron beam (or current) in a plasma situated in a magnetic mirror trap was used in many investigations to obtain a plasma with "hot" electrons [1-6]. In the past few years, linear and quasilinear theories of the electron instability of an electron beam in a plasma were developed [7-9] and subjected to experimental verification using pulsed electron beams. The agreement between theory and experiment was found to be satisfactory [10-11]. Much less progress was made in the theory [12-15] and experiment for stationary conditions (deep nonlinearity). A number of important problems concerning the mechanism of electron heating under stationary conditions (stochastic acceleration), the values of the density, temperature, the distribution functions for the hot electrons, etc. call for further clarification and refinement. Nor is there at present enough experimental material on the decay of a plasma with hot electrons situated in a magnetic trap, and the existing data [3,16,17] have not yet been adequately interpreted. The mechanism of anomalous decay, observed in a plasma with hot electrons, has likewise not been sufficiently investigated [6,17,18].

We present in this paper the results of experiments carried out with a setup similar to that used by Alexeff et al.[2] Our data yield additional information with respect to the characteristics of the stationary beam-plasma discharge situated in a magnetic field of mirror configuration, and the decay of the hot-electron plasma which is produced thereby.

2. DESCRIPTION OF INSTALLATION AND OF THE OPERATING MODES

To produce a plasma with hot electrons we used a discharge with an incandescent cathode and a neutral-gas pressure gradient [2], disposed along the axis of a magnetic mirror trap. A diagram of the setup is shown in Fig. 1. The two main solenoid windings 1, producing the mirror-configuration field, were placed in a vacuum container 2 of stainless steel, evacuated with diffusion pumps with a total capacity not less than 4,000 liters/sec of hydrogen. The residual pressure in the container was approximately 1×10^{-6} mm Hg. The magnetic field in the mirrors could reach values 5,000 Oe, and the field in the center of the trap was 1200 Oe. In one of the coils was located an electron gun consisting of an incandescent flat tantalum cathode 3 and a massive copper anode 4 with a round channel along its axis, of 10 mm diameter and 40 mm length. The working gas (in most experiments—hydrogen) was fed to the central part of the channel through a tube 5. The electron beam passed along the magnetic-trap axis and was incident on an anticathode. Both a solid anticathode 6, with disc diameter 35 mm, and an anticathode in the form of a hollow cylinder 7 with opening diameter 50 mm and length 90 mm, were used. When the hollow anticathode was used,

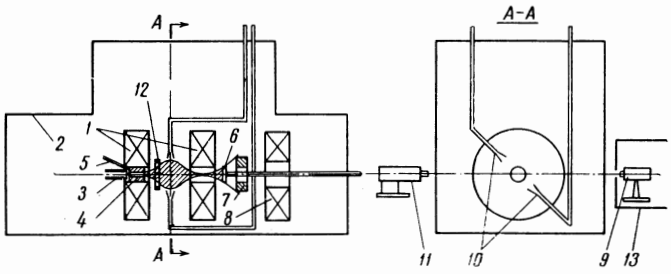

FIG. 1. Schematic diagram of the installation: 1 – coils producing the magnetic mirrors, 2 – vacuum container, 3 – cathode, 4 – anode, 5 – gas supply tube, 6 – solid anticathode, 7 – hollow anticathode, 8 – opposing-field coil, 9 – x-ray counter, 10 – microwave horns, 11 – monochromator, 12 – diamagnetic probe, 13 – lead shield.

the discharge was ignited by producing at the location of the anticathode, with the aid of an additional solenoid winding 8, an opposing magnetic field of several hundred Oe intensity. The discharge was fed from a low-resistance high-voltage source (U_{max} = 6—7 kV, I_{max} = 5—7 A), with negative voltage applied to the cathode. The anticathode could either be under a floating potential, or grounded through a ballast resistor. To produce the pulsed mode, an electronic voltage-modulation system was used. In most experiments, the voltage pulse duration was 10 msec and the pulse repetition frequency was 5 pulses/sec.

Depending on the physical parameters of the system, it was possible to excite two types of discharge: low-resistance arc or high-resistance discharge with x-radiation. The main physical parameters on which the type and intensity of the discharge depended were: gas pressure P, anode voltage, and magnetic field intensity H_0. The character of the excited discharge determined the value of such parameters as the anticathode voltage U_{ac}, the total current drawn from the power supply I_a, etc. The discharge depended also on the geometry of the electron gun, the position of the anticathode, the size of the ballast resistance in the anticathode circuit R_b, etc. The optimal conditions for the high-resistance discharge were chosen such to produce maximum density and temperature of the hot electrons.

The low resistance arc was excited at sufficiently high-hydrogen pressure in a container with $P > 10^{-4}$ mm Hg, low anode voltage U_a = 200—700 V ($U_{ac} \approx 0$), and the magnetic field could be varied in a wide range from 200 to 1200 Oe. The discharge was in the form of a well delineated braid in the shape of the magnetic-field force lines, with a diameter ~3 cm in the central part.

The high-resistance discharge with the x-radiation was observed at hydrogen pressures in the container $P \approx (6—10) \times 10^{-5}$ mm Hg and at anode voltages 2—3 kV and higher. To obtain a discharge with maximum x-ray intensity, the maximum magnetic field was used (H_0 = 1200 Oe), and the anode voltage was raised to 5—6 kV. The current drawn from the power supply reached 2—3 A, and the anticathode voltage was 3—3.5 kV. The discharge "fanned out" in the transverse direction to 10—15 cm. The maximum x-ray level on the outer side of the container walls (8—10 mm thick) reached 150—200 mr/hr (continuous mode). It should be noted that the operating mode of the installation (continuous or pulsed) had no influence on the characteristics of the discharge. The plasma parameters in the discharge pulse itself was the same as in the stationary discharge.

The results that follow pertain exclusively to the high-resistance discharge with x-radiation.

3. MEASUREMENT RESULTS

We used several diagnostic procedures to determine the characteristics of the stationary and decay plasma.

A. X-ray Measurements

The hot-electron plasma is a source of bremsstrahlung x-rays, making it possible to obtain information with respect to a number of physical quantities: the temperature of the hot electrons T_{eh}, their density n_h, the dimensions of the glowing region, and the lifetime in the magnetic trap τ.

1. The dimensions of the region occupied by the hot electrons were determined from x-ray photographs obtained with a pinpoint camera (Fig. 2). The photography was on special x-ray film through a window in the container, covered with an aluminum foil of 100 μ thickness. The photometry of the film with the plasma image yielded the following plasma dimensions: length 14 cm, and diameter of the central part 2.8 cm. (half-width of

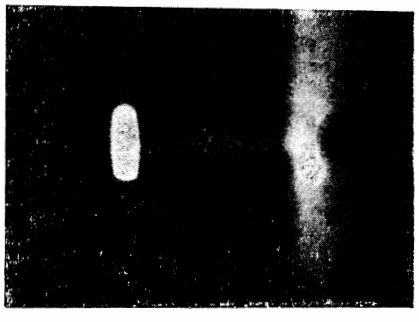

FIG. 2. X-ray photograph of discharge. The primary electron beam passes from left to right. In the right side of the figure is shown the image of the flange of one of the mirror coils.

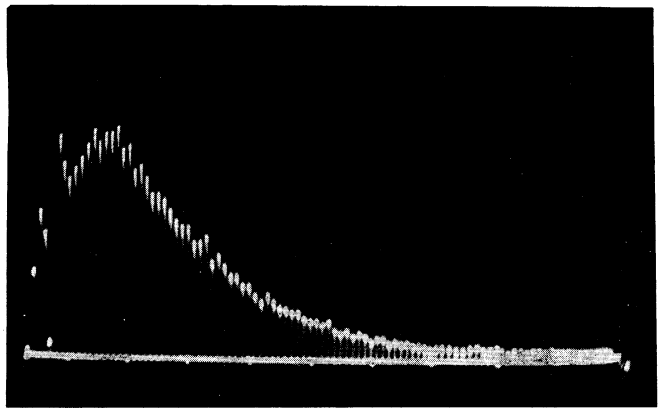

FIG. 3. Histogram of typical spectrum of the x-radiation from the plasma. The hundredth channel corresponds to energy E_γ = 500 keV.

the photometry curve). The plasma shape can be identified with an ellipsoid of revolution.

2. T_{eh} was determined from the energy spectrum of the bremsstrahlung quanta emitted by the central part of the volume. Collimation of the radiation was with the aid of diaphragms and lead shields. The container walls were 40 cm from the glowing volume. The emission spectrum was plotted with the aid of a scintillation γ spectrometer with NaI(Tl) crystal, photomultiplier (FÉU-29), and 100-channel pulse-height analyzer (AI-100-1, resolution time 40 + n μsec, n—channel number) for a single-channel differential discriminator (AADO-1), used for control measurements (resolution time $\approx$ 1 μsec).

Figure 3 gives the histogram of a typical plasma x-ray spectrum. The energy calibration was against the known spectrum of Cs^{137} with quantum energy E_γ = 661 keV.

To determine T_{eh}, the experimental spectrum was compared with a theoretical one calculated for a Maxwellian electron distribution [19]:

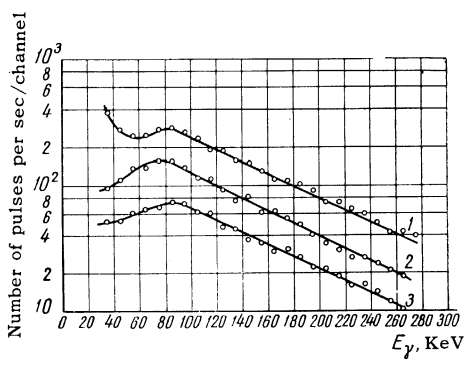

FIG. 4. Spectra of the bremsstrahlung from the plasma: 1 – discharge, 2 – decay 2 msec after the end of the discharge pulse, 3 – the same after 8 msec; $T_{eh} \approx$ 100 keV.

$$\left(\frac{dQ}{dE}\right)_{\text{theor}} = \frac{16}{3}\frac{r_0^2c^2}{137} n_h n_0 \sqrt{\frac{2m}{\pi T_{eh}}} \exp\left(-\frac{E_\gamma}{2T_{eh}}\right) K_0\left(\frac{E_\gamma}{2T_{eh}}\right). \quad (1)$$

The approximate value of T_{eh} was determined from the slope of the experimental curve $(dQ/dE)_{exp}$ in the quantum energy region $E_\gamma \geq T_{eh}$ plotted on a semilogarithmic scale. Figure 4 shows the characteristic spectra of the bremsstrahlung from the plasma of the discharge and of the decay part.

The energy resolution for the employed NaI crystal (diameter 40 mm, height 40 mm) is calculated to be 20% for E_γ = 100 keV and 25% for E_γ = 20 keV [20]. Corrections for the absorption of the quanta in the container window and in the crystal liner were introduced in the soft part of the spectrum. The total thickness of the absorber was equivalent to 0.5 mm of aluminum. The correction for the absorption of the 20-kV radiation was 35%.

3. The density of the hot electrons was determined by measuring the total energy flux from a known plasma volume, which in turn was determined by calculation. The calculated value of n_h was obtained from the known relation [19]:

$$Q = 1.69 \cdot 10^{-25} n_h n_0 T_{eh}^{1/2} (\text{erg/cm}^3 \text{ sec}). \quad (2)$$

Here N_0 is the density of the neutral atoms and T_{eh} the temperature in eV. For the most intense modes, n_h amounted to 1×10^{11} electrons/cm^3 (Q = 36 erg/cm^3 sec). We did not take into account the relativistic correction for the bremsstrahlung of electrons from electrons, which reaches ~30% for a Maxwellian distribution with $T_{eh} \approx$ 100 keV. Failure to take this correction into account overestimates the value of n_h given by (2). On the other hand, we did not register the radiation in the soft part of the spectrum (up to 20 keV), which underestimated the result calculated for a Maxwellian spectrum by ~20%. The main experimental error in the determination of n_h is connected with the uncertainty in the size of the radiating volume and is estimated at ± 25%.

4. Figure 5 shows an oscillogram of the x-rays registered with a scintillation counter in the absence of collimation. The dense "forest" of pulses corresponds to the discharge (duration 10 msec), followed by the decay part. On the decay part one can see two large pulses due to the superposition of a large number of quanta in a short time interval (the constant of the recording apparatus was 0.5 μsec). These pulses are gathered away by a lead absorber of 5 mm thick, located ahead of the scintillation counter, and re-

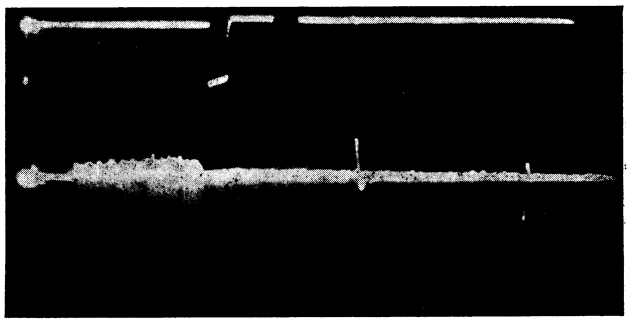

FIG. 5. Registration of x-ray flux by a scintillation counter. The afterglow shows two large pulses corresponding to anomalous plasma decay, 11 and 23 msec after the end of the discharge.

flect the anomalous decay of the plasma with the hot electrons.

B. Microwave Measurements

1. Determination of plasma density. The plasma was sounded with a microwave signal at 3.2 cm wavelength. The microwave system consisted of a generator, receiving and transmitting horns with apertures 35 × 35 mm, spaced 220 mm apart (see Fig. 1), a flow-through attenuator, and a detector section. The generator operated in a mode of internal modulation at 1 kHz. Figure 6 shows typical oscillograms of the signal passing through the plasma. In the most intense mode, practically complete blocking of the signal is observed (attenuation ≥ 20 dB), corresponding to a plasma density $n_e \geq n_{crit} = 1.1 \times 10^{12}$ el/cm^3. Under these conditions, apparently, the total plasma density n_e in the central part of the discharge did not greatly exceed n_{crit}, since the modes at which incomplete blocking of the signal was observed (Fig. 6b, attenuation ~ 14 dB), and complete blocking (Fig. 6a, attenuation ~ 20 dB), corresponded to nearly equal values of the physical parameters characterizing the discharge (P, U_a, H_0, U_{ac}, I_a, x-ray dosimeter readings, hardness of the x-rays, etc.).

After the end of the discharge pulse, an appreciable attenuation of the signal, ~3—5 dB (decay part), is still observed. Using the theory of refraction attenuation of a microwave signal in a plasma, neglecting geometrical optics [21], we can obtain data with respect to the plasma density in the decay part. The average value of the plasma density at the start of the decay (t = 0.3 msec) is (2.5—3) × 10^{11} el/cm^3, under the assumption that the plasma diameter is 3.0 cm (x-ray photograph data). The decay plasma, as a rule, is interrupted by an anomalous jump (see Figs. 6a and b). The threshold density that could be noticed is estimated at 10^{10} el/cm^3. It should be noted that in the continuous mode, the plasma density was determined in the 1.5 × 10^{11}—4 × 10^{11} el/cm^3 by two methods: by determining the attenuation and by determining the phase shift of the transmitted signal. Both methods are in satisfactory agreement within the limits of measurement accuracy (± 15%).

2. Radiation from plasma. The electromagnetic radiation from the plasma was received with a loop-type or rod-type coaxial probe introduced inside the container and located 10—20 cm from the visible boundary of the plasma. To register the radiation, commercial apparatus was used, SCh-5 frequency spectrum analyzer and P5-5 and TPS-54 receivers. In addition, in the 3- and 10-cm bands, we used broadband waveguide systems with detector sections.

The microwave radiation was registered only in the mode with the x-radiation. The intensity of

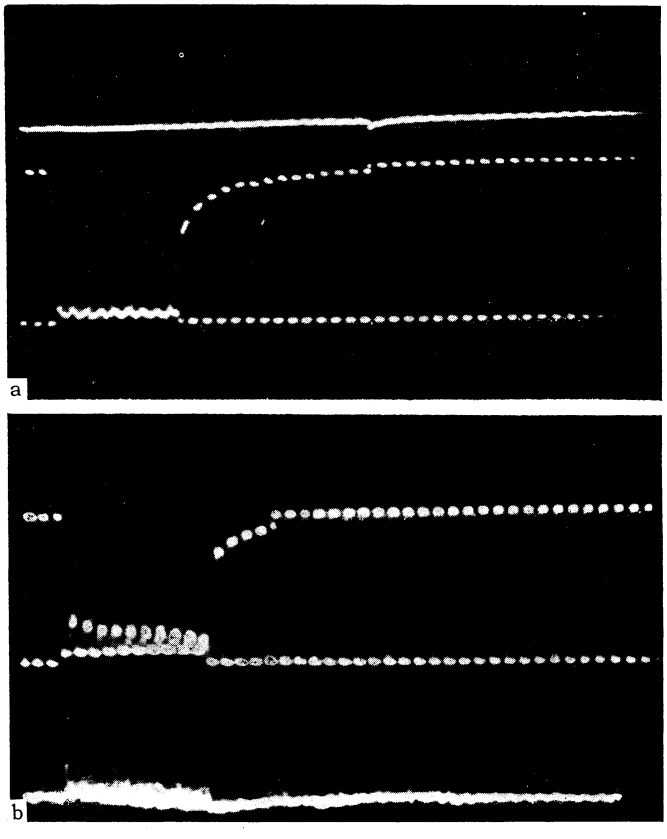

FIG. 6. Oscillograms of sounding microwave signal (3 cm) and radiation from the plasma. a – Lower trace – modulated microwave signal (each marker – 1 msec), attenuation during the discharge ~20 dB; upper trace – x-rays (small amplification); the anomalous decay at the 14th msec is observed. b – upper trace – microwave signal, attenuation at the end of the discharge pulse ~14 dB; lower trace – electromagnetic radiation from the plasma in the 10 MHz range: anomalous decay is seen at the 5th msec.

the oscillations increased with increasing x-ray emission. On the decay part of the pulsed mode, there was no radiation (Fig. 7a). In the 1500—7400 MHz band, a continuous spectrum was observed with individual peaks of width up to 20 MHz. The most intense peaks corresponded to frequencies 3400, 3800, 4120, 5500, and 5650 MHz. The radiation was registered at the 10^{-7}—10^{-8} W level. The maximum excess of the signal over the average noise level was 10 dB. The positions of the peaks did not depend on the magnetic field. Figure 7b shows a typical oscillogram of the radiation peak at 4,920 MHz. The TPS-54 receiver registered in the 10—18 MHz band the electromagnetic radiation corresponding to the instant of the anomalous decay of the plasma (narrow peak on the low oscillogram of Fig. 6b).

C. Optical Measurements

An appreciable part of the radiation for the plasma was in the optical band, making it possible to carry out certain optical measurements.

1. Relative line intensity. To register the light from the plasma we used a UM-2 monochromator with FÉU-29 photomultiplier, the current of which was measured with a meter (continuous mode) or with an oscilloscope (pulsed mode). The natural time constant of the apparatus does not exceed

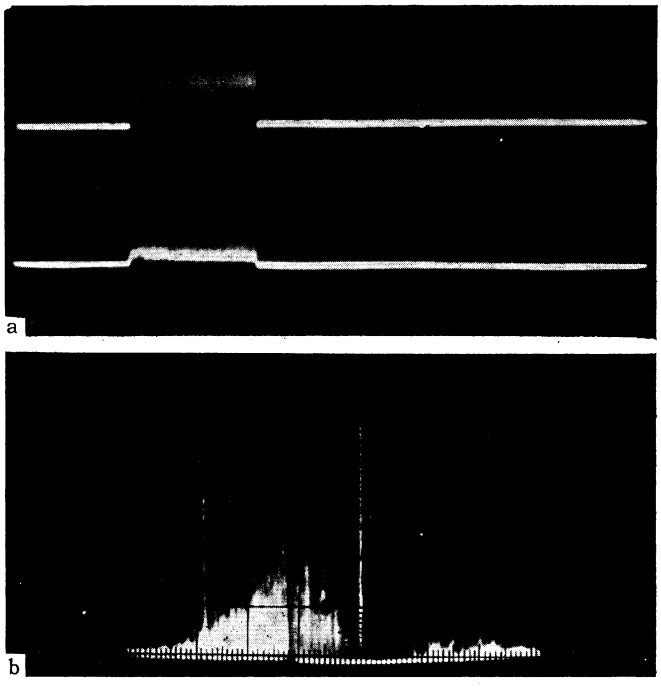

FIG. 7. Oscillogram of microwave radiation from the plasma. a – Upper trace – signal from P5-5 receiver (f = 3800 MHz); lower trace – signal of three centimeter detector section (time sweep); b – signal from S4-5 frequency spectrum analyzer (f = 4,120 MHz).

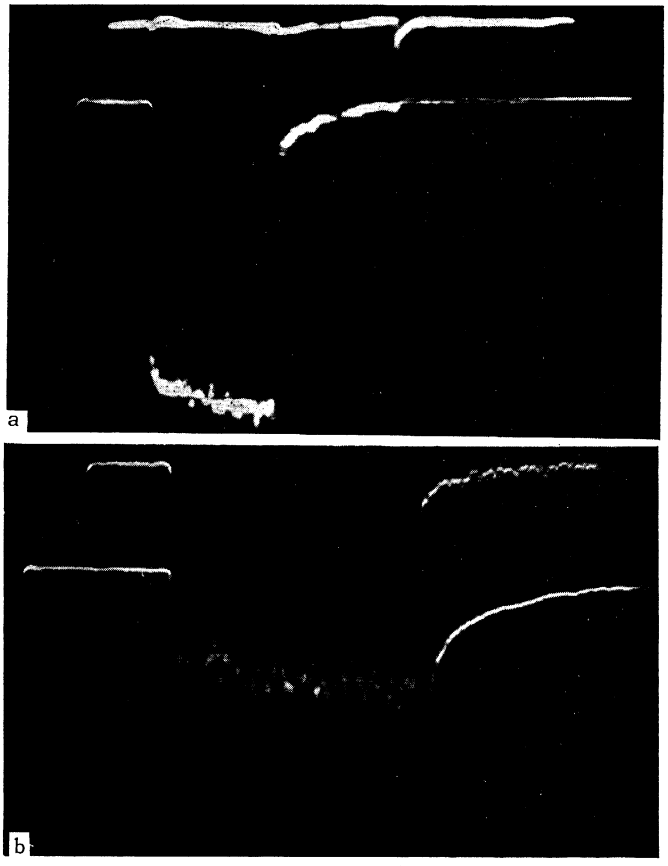

FIG. 8. Oscillogram of the intensity of the spectral lines and of the total light. a – Lower trace – H_β line, discharge pulse duration 10 msec; upper trace – x-rays. Anomalous decay at the tenth msec. b – Upper trace – line He I (λ = 5015 Å), lower trace – total light.

0.1—0.2 msec. In some of the experiments, the total light flux was registered. For registration with the monochromator, we chose the atomic hydrogen H_β line, and also the helium line He I (λ = 5015 Å—singlet, λ = 5875 Å—triplet), measured batches of which were specially introduced into the discharge. Figure 8 shows typical oscillograms of the intensities of the H_β and He I (λ = 5015 Å) lines and of the total light. The reduction of the oscillograms shows that the intensities of the H_β and He I (λ = 5015 Å) lines decreases after the end of the discharge pulse by a factor 6—8, and that of the He I (λ = 5,875 Å) line by a factor of 40—50. The discharge pulse is followed by a region of smooth drop in intensity. The ratio of the intensities of the He I lines (5015/5875) in the discharge pulse turned out to be 0.3—0.4, and on the decay part it turned out to be 2—2.5 regardless of the instant of time, within the limits of the measurement accuracy (± 30%). (In the stationary discharge in the low-resistance arc mode, this ratio 0.08—0.09, corresponding to T_e = 13—15 eV.)

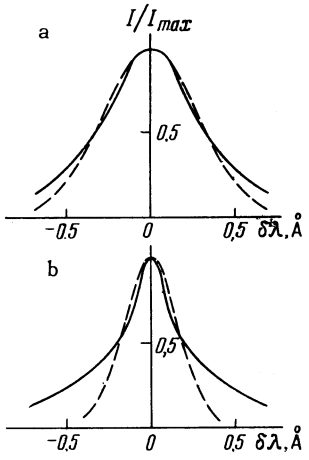

FIG. 9. Contours of the H_β line. Solid curve – experiment, dashed – Doppler contour.

The oscillograms of the line intensities show for different instants of time on the decay certain steps reflecting the anomalous decay of the plasma, in which the glow decreases by a factor 5—7. The instant of appearance of the step is strictly correlated with the burst of x-radiation (see Fig. 8a) and the anomalous jump in the attenuation of the sounding microwave signal.

2. Width of spectral lines. To obtain the line contours we used a Fabry-Perot interferometer (IT-51), crossed with a spectrograph (ISP-51) with a camera having f = 270 mm. We studied the contours of the lines $H\beta$, H_γ, H_δ, He I, and He II. The lines have noticeable broadening. The half-width of the $H\beta$ lines ranges from 0.4 to 1.2 Å, corresponding to a neutral-atom temperature of 1.5—13.5 eV, assuming Doppler broadening. Figure 9 shows typical contours of the $H\beta$ lines when light is recorded from the entire volume of the plasma (a) and when sighting on the central region (b). As seen from the figure, in the case when the radiation from the central region is recorded, noticeable deviation of the line contour from the Doppler line contour is observed. It should be noted that this line broadening is not typical of the x-radiation mode alone, and is observed also in the low-resistance arc.

D. Diamagnetic Measurements

The hot-electron plasma has a noticeable diamagnetic effect, from which one can determine the density of the transverse particle energy $W_\perp = n_e T_e$. The measurements were made with the aid of a probe in the form a coil with inside diameter 100 mm, containing 500 turns of copper wire (0.15 mm diameter). The coil was enclosed in a metallic screen protecting the probe against induction. The probe was moved perpendicular to the discharge axis at a distance 35 mm from the central plane, and subtended the plasma column. Figures 10a and b show oscillograms of the voltage picked off the probe. The first pulse in the oscillograms occurs when the discharge is ignited and is connected with the generation of plasma with hot electrons. The second pulse reflects the decay of the plasma after the termination of the discharge pulse. The area under the pulses characterizes the energy contained in the plasma. The value of $W_\perp$ was calculated from the relation

$$W_\perp\left(\frac{\text{eV}}{\text{cm}^3}\right) = \frac{0.5\cdot 10^{19}\cdot H_3}{w_3 S_{\text{эeff}}}\int_0^\infty \varepsilon(t)\,dt, \qquad (3)$$

where H_{pr} is the intensity of the constant magnetic field in the vicinity of the probe, equal to 1650 Oe at H_0 = 1200 Oe, w_{pr} = 500 turns, and S_{eff} is the effective area of the radiating plasma at the probe location. This area was determined from the x-ray photograph of the plasma and turned out to be 5.3 cm^2. $\epsilon(t)$ is the voltage picked off the probe, in volts.

Relation (3) was verified in special experiments with a working model of the probe using exponential magnetic-field calibration pulses produced with the aid of a solenoid imitating the plasma. The calculations and the measurements of the calibration field coincide within the measurement

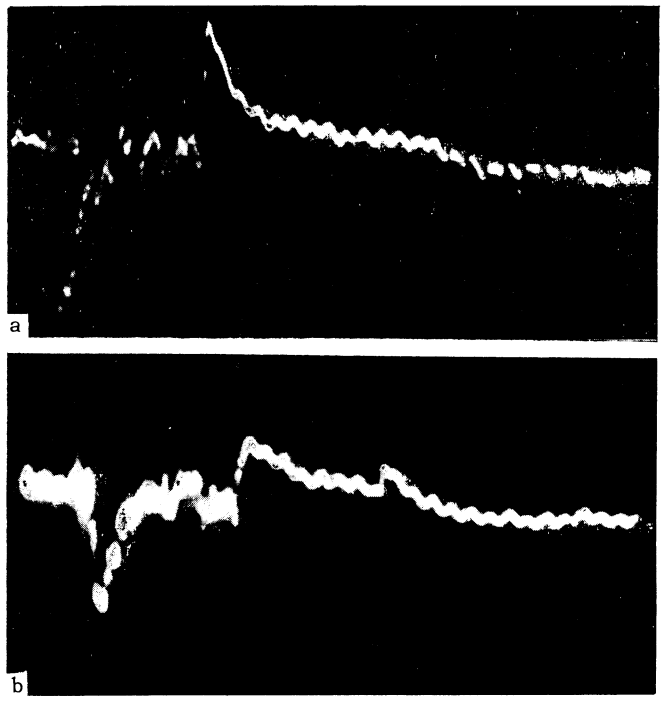

FIG. 10. a – Oscillogram of voltage from diamagnetic probe; b – the same, showing the anomalous decay at the 10th msec. Oscillations with frequency 730 Hz correspond to pulsations of the main magnetic field.

accuracy (~ 5%) for exponential pulses with decay constants $\tau \leq 3$ msec. Since an appreciable fraction of the plasma (up to 60%) decayed under our conditions within a time not exceeding 3 msec, the use of relation (3) to determine the energy content of the plasma does not give rise to appreciable errors (less than 10%).

Substantial difficulties in the measurement of the diamagnetic signal were due to pulsations of the magnetic field at low frequencies (10—12 and 730 Hz), connected with the operation of the dc generator feeding the main coils. The total error in the determination of the area under the diamagnetic-signal curve is estimated at ± 10%. The mean energy content for the intense mode was 6×10^{15} eV/cm^3.

At the instant of anomalous plasma decay, a second diamagnetic pulse is observed on the oscillogram. The energy content of the anomalous pulse is estimated at 10—40% of the initial stored energy, in agreement with the x-ray measurements.

4. DISCUSSION OF THE RESULTS

1. Comparison of the results of an independent determination of the energy content of the plasma ($n_e T_e$) as made with x-ray and diamagnetic measurements for the same experiments show them to be in satisfactory agreement. Thus, according to x-ray measurements, $n_h = 1 \times 10^{11}$ electron/cm^3 and $T_{eh} \approx 70$ keV ($n_h T_{eh} \approx 7 \times 10^{15}$ eV/cm^3), and according to the diamagnetic signal $n_e T_{e\perp} \approx 6 \times 10^{15}$ eV/cm^3. The agreement between the results of the x-ray and diamagnetic measurements points to a definite degree of reliability of the data on n_h and T_{eh}, and also to the small role played by the impurities and by release of gas from the container walls in the discharge.

It follows from the results of x-ray and microwave measurements of the density that in a stationary discharge (or in a discharge pulse) the fraction of the hot electrons in the central region of the discharge amounts to approximately 1/10 of the total density, and rises to 1/3 on the decay part.

2. Figure 11 shows a comparison of the experimental results of the energy distribution of the x-ray radiation from a plasma, with the theoretical curve for a Maxwellian electron velocity distribution. This figure shows both our experimental data and the data of [2]. The agreement between the experimental spectrum and the theoretical in the quantum energy region $E_\gamma/T_{eh} > 0.5$ can be regarded as confirmation of the

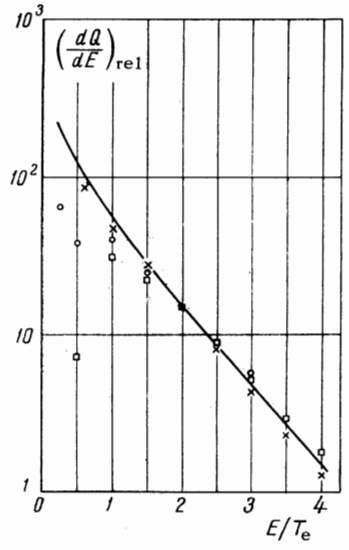

FIG. 11. Comparison of the experimental and theoretical spectrum of x-rays from the plasma. Solid curve – theoretical spectrum for Maxwellian electron distribution [19]. Experimental data of the plasma discharge: + – T_{eh} = 25 keV, our result; o – T_{eh} = 100 keV, our results; □ – T_{eh} = 130 keV, results of [2]. The experimental points and the theoretical curve are aligned at $E/E_{eh} = 2$. The ordinates represent $(dQ/dE)_{rel}$ – the relative intensity of the bremsstrahlung per unit energy interval.

assumption concerning the stochastic acceleration of the electrons in the stationary discharge.

3. The appreciable decrease in the attenuation of the microwave signal and of the intensity of the spectral lines after the end of the discharge pulse, within a time of the order of hundreds of microseconds (see the oscillograms of Figs. 6 and 8) are evidence that a large group of relatively cold electrons move out of the magnetic trap. From a comparison of the x-ray and microwave measurements of the electron density it follows also that the bulk of the electrons in the discharge remain cold. We have no direct experimental data with respect to the energy distribution of the electrons in the region of small and intermediate energies up to 15—20 keV. We present below certain considerations and calculations with respect to the possible composition of the plasma electrons both on the decay part and in the discharge itself; these are corroborated by optical and other measurements.

Decay plasma. In view of the presence, of a considerable density of neutral hydrogen ($n_0 = 3.5 \times 10^{12}$ molecules/cm^3 or 7×10^{12} atom/cm^3, in the space between the solenoid windings, secondary electrons will be emitted in the volume occupied by the primary plasma with the hot electrons as a result of ionizing collisions with the

neutral particles. A certain fraction of these secondary electrons, having an energy exceeding the hydrogen ionization threshold, can participate in further ionization acts, although their average energy does not exceed 10—15 eV [22]. As a result of this process and of the scattering of the electrons in the magnetic-trap volume initially occupied by the hot electrons, a quasi-equilibrium concentration of the primary (hot), secondary, and tertiary electrons, having energies below the ionization threshold and an average energy of approximately 2.5 eV, will become established.

The relative concentration of the indicated electron groups (n_h, n_2, n_3) is determined from the following relations:

$$\frac{n_h}{n_2} = \frac{1}{2R}\frac{\langle\sigma_{el}v\rangle_2}{\langle\sigma_i v\rangle_h} + \frac{\langle\sigma_i v\rangle_2}{\langle\sigma_i v\rangle_h}, \quad (4)$$

$$\frac{n_3}{n_2} = 4R\frac{\langle\sigma_i v\rangle_2}{\langle\sigma_{el}v\rangle_3}, \quad (5)$$

where $R = H_{mir}/H_0$ is the mirror ratio, σ_{el} the effective cross section for elastic electron collisions, σ_i the effective ionization cross section, and $\langle\sigma v\rangle$ a quantity characterizing the rate of the corresponding process, averaged over the electron velocity distribution. Expressions (4) and (5) are valid under the assumption that the departure of the electrons from the trap is due principally to elastic collisions with neutral particles, and that the following relation holds true for lifetimes $\tau_h \gg \tau_2$ and $\tau_h \gg \tau_3$ of the indicated electron groups. By substituting in (4) and (5) R = 4.2 and the following quantities: $\langle\sigma_i(H_2)v\rangle_h \approx 2\langle\sigma_i(H)v\rangle_h = 1.4\times10^{-8}$ cm^3/sec, $\langle\sigma_i(H_2)v\rangle_2 \approx 1.5\langle\sigma_i(H)v\rangle_2 = 2.1\times10^{-8}$ cm^3/sec, and $\langle\sigma_{el}(H_2)v\rangle_{2,3} \approx \langle\sigma_{el}(H)v\rangle_{2,3} \approx 1.3\times10^{-7}$ cm^3/sec,[1)] obtained for the hot electrons (T_{eh} = 100 keV) by averaging over the Maxwellian distribution and for the remaining electron groups by averaging over the theoretical distribution of Mott and Massey [22], we obtain for the relative densities $n_2/n_h = 0.29$ and $n_3/n_h = 0.55$ for atomic hydrogen and $n_2/n_h = 0.3$ and $n_3/n_h = 1.2$ for molecular hydrogen.

The group of secondary and tertiary electrons can be combined into a single common group of cold electrons with relative concentration $n_c/n_h = (n_1 + n_2)/n_h = 0.75$ for atomic hydrogen and 1.5 for molecular hydrogen. The latter value is in good-agreement with microwave measurements of $n_e = n_c + n_h$ and measurements of n_h in the x-ray region ($n_e/n_h \approx 2.5$—3). The average energy of the cold-electron group is 4—5 eV.

The calculation is also in good agreement with additional optical measurement data. The singlet-to-triplet ratio of the He I line intensities is given by

$$\frac{I_{5015}}{I_{5875}} = \frac{\nu_s}{\nu_t}\frac{n_h\langle\sigma_s v\rangle_h + n_c\langle\sigma_s v\rangle_c}{n_h\langle\sigma_t v\rangle_h + n_c\langle\sigma_t v\rangle_c} \approx 1.17\frac{n_h}{n_c}\frac{\langle\sigma_s v\rangle_h}{\langle\sigma_t v\rangle_c}. \quad (6)$$

Equation (6) can be simplified, since under our conditions $\langle\sigma_s v\rangle_h = 3.3\times10^{-12}$, $\langle\sigma_s v\rangle_c = 2.5\times10^{-14}$, $\langle\sigma_t v\rangle_c = 0.8\times10^{-12}$, and $\langle\sigma_t v\rangle_h \approx 2\times10^{-14}$ (see footnote [1)]).

The ratio I_{5015}/I_{5875} is sufficiently sensitive to the choice of T_{ec} in the investigated region of cold-electron temperatures (1—10 eV). The experimental value of I_{5015}/I_{5875} ranges between 2.0 and 2.5, which is in good agreement with the calculated value $n_c/n_h = 1.5$ and T_{ec} = 4 eV. We can thus regard it as established that a decay plasma contains two groups of electrons: a hot group with $T_{eh} \approx 100$ keV and relative density $n_h/n_e \approx 0.4$, and a cold group, which is in equilibrium with the hot one, with average energies ~ 4 eV, $n_c/n_e \approx 0.6$, and with a near-Maxwellian summary distribution.

Discharge plasma. We chose as the working hypothesis the assumption that the plasma of a discharge pulse contains three electron groups with Maxwellian distribution: hot with $T_{eh} \approx 100$ keV, warm with $T_{ew} \approx 100$ eV, and cold with $T_{ec} \approx 4$ eV. For the relative density of the hot components we assumed the experimental value $n_h/n_e = 0.1$ ($n_e = n_h + n_w + n_c$). The relative densities of the two other groups were calculated from relations similar to (4) and (5), which take into account the formation of a cold component due to ionization of the neutral particles by the warm and hot electrons, and turned out to be $n_w/n_e \approx 0.1$ and $n_c/n_e \approx 0.8$.

a. The ratio of the intensities of the He I lines in the discharge can be expressed, in accord with the foregoing hypothesis, in the form

$$\frac{I_{5015}}{I_{5875}} = \frac{\nu_s}{\nu_t}\frac{n_c\langle\sigma_s v\rangle_c V_c + n_w\langle\sigma_s v\rangle_w V_w + n_h\langle\sigma_s v\rangle_h V_h}{n_c\langle\sigma_t v\rangle_c V_c + n_w\langle\sigma_t v\rangle_w V_w + n_h\langle\sigma_h v\rangle_h V_h}. \quad (7)$$

Let V_c, V_w, and V_h be the radiating volumes occupied by the respective electron groups. Introducing the relation $V_c \approx 4V_h$, which follows from a comparison of the ordinary and x-ray photographs of the discharge, making the natural as-

[1)] In calculating the quantities $\langle\sigma v\rangle$, we used the cross sections for ionization and elastic scattering in H and H_2, and excitation of the lines He I and H_β given in [23,24]. We used the Born-approximation formulas (see, for example, [25] for the cross sections for ionization and excitation of the singlet lines at high energies, and estimated the excitation of the triplet He I line by hot electrons by extrapolating the experimental data, which obey the 1/E law [24,25], to the region of high energies (E > 400 eV).

sumption $V_w \approx V_h$, substituting the values $\langle \sigma_s v \rangle_w = 1.5 \times 10^{-11}$ cm^3/sec and $\langle \sigma_t v \rangle_w = 4.8 \times 10^{-11}$ cm^3/sec and the remaining values of $\langle \sigma_v \rangle$ (see the section headed "Decay plasma"), and neglecting the contribution of the inessential terms, we obtain the simplified expression

$$\frac{I_{5015}}{I_{5875}} \approx \frac{\nu_s}{\nu_h} \frac{\langle \sigma_s v \rangle_w}{\langle \sigma_t v \rangle_w}. \quad (8)$$

The experimental value of the ratio of the intensities was 0.3—0.4, corresponding to a temperature of 70—130 eV for the warm group.

b. The ratio of the intensities of the same He I line on going from a discharge pulse to the initial instant of decay is expressed for the triplet by the formula

$$\frac{I^p_{5875}}{I^d_{5875}} = \frac{n_c^p \langle \sigma_t v \rangle_c V_c^p + n_w^p \langle \sigma_t v \rangle_w V_w^p + n_h^p \langle \sigma_t v \rangle_h V_h^p}{n_c^p \langle \sigma_t v \rangle_c V_c^p + n_h^d \langle \sigma_t v \rangle_h V_h^d}. \quad (9)$$

A similar expression holds for the singlet with the corresponding values of $\langle \sigma v \rangle$. Substituting the values of $\langle \sigma v \rangle$, introducing the relations $V^p_w \approx V^p_h = V^d_h = V^d_c$, and $V^p_c \approx 4V^d_c$, and neglecting the contribution of the inessential terms in (9) we obtain:

1) for the triplet

$$\frac{I^p_{5875}}{I^d_{5875}} \approx \frac{n_c^p}{n_c^d} \frac{V_c^p}{V_c^d} + \frac{n_w^p}{n_c^d} \frac{\langle \sigma_t v \rangle_p}{\langle \sigma_t v \rangle_c} \approx 4 \frac{n_c^p}{n_c^d} + 60 \frac{n_w^p}{n_c^d}, \quad (10)$$

2) for the singlet

$$\frac{I^p_{5015}}{I^d_{5015}} \approx 1 + \frac{n_w^p}{n_h^d} \frac{\langle \sigma_s v \rangle_w}{\langle \sigma_s v \rangle_h} = 1 + 4.6 \frac{n_w^p}{n_h^d}. \quad (11)$$

The ratio of the H_β intensities is governed by an expression of the type (11) with a coefficient 5.9 preceding n^p_w/n^d_h.

The results of the calculations and the experimental values of the line intensity ratios are summarized in the Table. We see from the table that the agreement between the experimental data and the calculation is satisfactory, thus confirming the assumed presence of three groups of electrons in the plasma of the investigated discharge.

We turn now to the temporal characteristics of the decay plasma. The oscillograms of the microwave signal and the intensities of the spectral lines (or of the integral light) consist of the following main regions: i) a plateau, reflecting the conditions of the stationary discharge; ii) a drop, lasting several hundred microseconds, due to the departure of cold and warm electrons from the trap; iii) a smooth decay part, the duration of which ranges from 0 to 10—15 msec, which is completed as a rule by an anomalous burst followed apparently by normal decay.

Line intensity ratio	Calculation	Experiment
I^p_{5875}/I^d_{5875}	60	40—50
I^p_{5015}/I^d_{5015}	5,6	6—8
I^p_β/I^d_β	6,9	6—8

Figure 12 gives normalized data on the total plasma density $n_e(t)/n_e(0)$, the spectral line intensity $I(t)/I(0)$, and the average hot-electron density $n_h(t)/n_h(0)$ (several points) for the decay region iii). As seen from the figure, the decay has a nonexponential form and can be characterized by a decay constant $\tau(t)$ for the exponential approximating the experimental curve as an arbitrary instant of time t. For all the experimentally obtained curves, similar to that shown in Fig. 12, $\tau(t)$ ranges from 1—3 msec for the start of the decay ($t = 0$) to 8—15 msec at $t = 10$ msec. The agreement in the character of the indicated curves (microwaves, light, x-rays) also confirms the assumption that the plasma has in the decay part a fundamental (hot) component and an accompanying (cold) electronic component. We note also that a noticeable decrease in the decay constant $\tau(t)$ from (8—10) to 3—4 msec) is observed ahead of the anomalous decay on some oscillograms of the microwave signal and of the line intensities.

The nonexponential nature of the decay in region iii) calls for additional research. It follows from Fig. 4 that during the decay the character of the x-ray spectrum and the temperature of the hot electrons remain practically constant, thus excluding the possibility of attributing the nonexponential nature to distortion of the form of the spectrum. (It is observed that the spectrum becomes harder in the region beyond the anomalous decay, where the temperature of the hot electrons increases by approximately 1.5 times, reaching

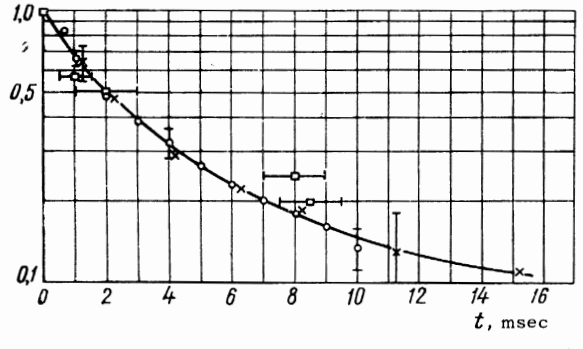

FIG. 12. Drop in the plasma density and in the intensity of the lines in the decay: × – total density $n_e(t)/n_e(0)$ (microwave measurements), □ – density of hot electrons $n_{eh}(t)/n_{eh}(0)$ (x-ray measurements), ○ – intensity of spectral lines $I(t)/I(0)$.

150 keV.) The nonexponential nature of the decay may possibly be due to the influence of the form of the magnetic field of the trap in the mirrors (non-adiabaticity) on the departure of particles from the trap [16].

The experimental value of $\tau(t)$ obtained in our experiments during the 10th—15th millisecond of the decay approaches the theoretical containment time of a plasma with hot electrons, which amounts to ~ 20 msec for T_{eh} = 100 keV, a neutral hydrogen density $n_0 = 7.4 \times 10^{12}$ at/cm^3, and a mirror ratio R = 4.2.

The authors are deeply grateful to B. K. Shembel' and V. S. Imshennik for interest in the work and a discussion of the results.

[1] M. V. Babykin, P. P. Gavrin, E. K. Zavoĭskiĭ, L. I. Rudakov, and V. A. Skoryupin, JETP 47, 1597 (1964), Soviet Phys. 20, 1073 (1965).

[2] I. Alexeff, R. V. Neidigh, and W. F. Peed, Phys. Rev. 136, A689 (1964).

[3] L. D. Smullin and W. D. Getty, Conference on Plasma Physics and Controlled Fusion Research, Culham, CN-21/122, 1965.

[4] P. I. Blinov, L. P. Zakatov, A. G. Plakhov, R. V. Chikin, and V. V. Shapkin, JETP Letters 2, 426 (1965), transl. p. 264.

[5] R. A. Demirkhanov, A. K. Gevorkov, A. F. Popov, and G. L. Khorasanov, op. cit.[3], paper CN-21/194.

[6] V. A. Simonov, V. V. Abozovik, and V. V. Ignat'ev, op. cit.[3], paper CN-21/167.

[7] Ya. B. Fainberg, Atomnaya énergiya 11, 313 (1961).

[8] V. D. Shapiro, JETP 44, 613 (1963), Soviet Phys. JETP 17, 416 (1963).

[9] A. A. Vedenov, E. P. Velikhov, and R. Z. Sagdeev, UFN 73, 701 (1961), Soviet Phys. Uspekhi 4, 332 (1961).

[10] I. F. Kharchenko, Ya. B. Faĭnberg, E. A. Kornimov, R. M. Nikolaev, E. I. Lutsenko, and N. S. Pedenko, JETP 38, 685 (1960), Soviet Phys. JETP 11, 493 (1960).

[11] A. K. Berezin, Ya. B. Faĭnberg, L. I. Bolotin, G. P. Berezina, I. Ya. Bez'yazychnyĭ, Yu. M. Lyapkalo, and E. V. Lifshitz, op. cit.[3], paper CN-21/181.

[12] Ya. B. Faĭnberg, F. G. Bass, and V. D. Shapiro, JETP 49, 329 (1965), Soviet Phys. JETP 22, 230 (1966).

[13] B. B. Kadomtsev, Voprosy teorii plazmy (Problems in Plasma Theory), no. 4, Atomizdat, 1964.

[14] T. H. Stix, Phys. of Fluids 7, 1960 (1964).

[15] P. A. Sturrock, Phys. Rev. 141, 186 (1966).

[16] V. I. Blinov, L. P. Zakatov, A. G. Plakhov, R. V. Chikin, and V. V. Shapkin, JETP Letters 3, 256 (1966), transl. p. 163.

[17] V. V. Alikaev, V. M. Glagolev, and S. A. Morozov, op. cit.[3], paper CN-21/5.

[18] L. A. Ferrari and A. F. Kuskes, Phys. of Fluids 8, 2295 (1965).

[19] V. I. Kogan and A. B. Migdal, R Fizika plazmy i problema upravlyaemykh termoyadernykh reaktsiĭ (Plasma Physics and the Problem of Controlled Thermonuclear Reactions), 1, AN SSSR, 1958.

[20] Yu. A. Egorov, Stsintillyatsionnyĭ metod spektrometrii gamma-izlucheniya i bystrykh neĭtronov (Scintillation Method of Spectrometry of Gamma Rays and Fast Neutrons), Atomizdat, 1963.

[21] M. A. Heald, The Application of Microwave Techniques to Stellarator Research, MATT-17, Aug. 26, 1959.

[22] N. F. Mott and H. S. W. Massey, Theory of Atomic Collisions, Oxford, 1933.

[23] Atomic and Molecular Processes, D. Bates, ed. (Russ. Transl.) Mir, 1964.

[24] S. É. Frish, Opticheskie spektry atomov (Optical Spectra of Atoms), Fizmatgiz, 1964.

[25] H. S. W. Massey and E. H. S. Burhop, Electronic and Ionic Impact Phenomena, Oxford 1962.

Translated by J. G. Adashko
7